

Journal of Materials Chemistry B

Accepted Manuscript



This is an *Accepted Manuscript*, which has been through the Royal Society of Chemistry peer review process and has been accepted for publication.

Accepted Manuscripts are published online shortly after acceptance, before technical editing, formatting and proof reading. Using this free service, authors can make their results available to the community, in citable form, before we publish the edited article. We will replace this *Accepted Manuscript* with the edited and formatted *Advance Article* as soon as it is available.

You can find more information about *Accepted Manuscripts* in the [Information for Authors](#).

Please note that technical editing may introduce minor changes to the text and/or graphics, which may alter content. The journal's standard [Terms & Conditions](#) and the [Ethical guidelines](#) still apply. In no event shall the Royal Society of Chemistry be held responsible for any errors or omissions in this *Accepted Manuscript* or any consequences arising from the use of any information it contains.



A multi-responsive intrinsically disordered protein (IDP)-directed green synthesis of fluorescent gold nanoclusters

Rajkamal Balu,^a Laure Bourgeois,^b Christopher M. Elvin,^c Anita J. Hill,^d Namita R. Choudhury^a and Naba K. Dutta^a

Received 00th xxx 2015,
Accepted 00th xxx 2015

DOI: 10.1039/x0xx00000x

www.rsc.org/

Herein we demonstrate the green synthesis of fluorescent gold nanoclusters (AuNCs) using a multi-responsive intrinsically disordered protein (IDP) polymer, Rec1-resilin as multi-functional template. Under controlled environment, Rec1-resilin acts simultaneously as the directing agent and the reducer, and performs the role of a highly efficient stabilizer once AuNCs are formed. In-depth understanding on the evolution of the photophysical properties and the chemical state of AuNCs formed are measured using UV-Vis, fluorescence and X-ray photoelectron spectroscopy. Circular dichroism (CD) spectroscopy measures the intrinsically disordered nature of Rec1-resilin stabilizing AuNCs. High resolution scanning transmission electron microscopy (STEM) reveals the three-dimensional (3D) structure of generated AuNCs of <1.5 nm size. A local ordering resembling that of a face-centered cubic (FCC) structure with evidence of twinning was observed for the generated AuNCs. The AuNCs so formed exclude the use of toxic reducing agents and displays excellent water dispersibility, photostability and environmental stability towards aggregation.

Introduction

In recent years, intense research interest has been focused on ultra-small metal nanoclusters (MNCs – metal nanoparticles (NPs) with diameter <2 nm) that exhibit fascinating physicochemical properties with promising applications in a wide range of fields including photonics, catalysis, sensing, and medicine.¹⁻⁴ Amongst other metals, gold nanoclusters (AuNCs) have been the subject of extensive investigation. During the last decade, a large variety of bottom-up and top-down techniques including simple chemical reduction, seed-mediated growth, photochemistry, electrochemistry, sonochemistry, template-assisted synthesis, supramolecular arrangements, lithography and galvanic replacement have been used to synthesize size and shape controlled AuNPs.²⁻⁴ However, the sub-nanosized regime remains relatively little explored.^{5, 6} Recently, concurrent theoretical and experimental research on size-selected AuNCs, prepared using surface deposition techniques, (e.g. vacuum evaporation, laser vaporization or magnetron sputtering and mass filtering under controlled conditions) have provided invaluable information on the electronic structure, cluster morphology and its evolution with the sizes of AuNCs.^{7, 8} In MNCs, when the size becomes comparable to

the Fermi wavelength of the electron the quantization effect leads to the evolution of the continuous conduction band to discrete energy levels.⁹ AuNCs with sizes comparable to the Fermi wavelength of electrons (<2 nm) behave like molecules and exhibit discrete electronic properties such as fluorescence with emission wavelength in correlation to the number of atoms in the cluster.¹⁰ The emission from molecular AuNCs is hypothesized to arise from both radiative interband (sp<d) transitions for high-energy visible fluorescence and radiative intraband (sp<sp) recombinations for low-energy near-infrared (NIR) emission across the HOMO-LUMO gap.¹¹ Over the last decade, facile and scalable solution phase synthesis of fluorescent AuNCs has been attempted by various modified Brust–Schiffrin methods using different templates or capping molecules including thiolates, dendrimers, oligonucleotide, polyelectrolyte, and synthetic polymers.^{2, 12} The controllability between AuNPs and fluorescent AuNCs synthesis can be obtained effectively by adjusting the experimental parameters, such as the metal to ligand ratio, pH of the solution, chemical structure and size of the ligands, the nature of the reducing agent, reaction temperature and time, etc.² Xie *et al.* first reported the synthesis and stabilization of fluorescent AuNCs using the globular protein bovine serum albumin (BSA) as molecular manipulator.¹³ Such protein-protected AuNCs are attractive and advantageous over other systems for their high water dispersibility, ease of bioconjugation and high biocompatibility.^{14, 15} However, AuNCs stabilized by protein have so far been demonstrated only using globular proteins and peptides with sulfur containing amino acids (cysteine and methionine), where the nucleated cluster were reported to be stabilized through broken disulfide bonds.¹³⁻¹⁵ The protein size was observed to be a critical factor for the photostability and long-term aqueous dispersibility of AuNCs.¹⁶

^a Ian Wark Research Institute, University of South Australia, Mawson Lakes, SA 5095, Australia. E-mail: naba.dutta@unisa.edu.au; namita.choudhury@unisa.edu.au

^b Monash Centre for Electron Microscopy, Department of Materials Engineering, Monash University, Clayton, VIC 3800, Australia.

^c CSIRO Agriculture, Level 6, Queensland Bioscience Precinct, St Lucia, QLD 4067, Australia.

^d CSIRO Manufacturing, Bayview Ave, Clayton, VIC 3168, Australia.

† Electronic Supplementary Information (ESI) available: See DOI: 10.1039/x0xx00000x

Moreover, the atomic structures of ligand-protected AuNCs are reported to be tightly correlated with the interfacial bond structure and the nature of the ligand interactions.¹⁷

Here we report the first study of an intrinsically disordered protein (IDP)-directed green synthesis and stabilization of fluorescent, water-dispersible and robust AuNCs (Fig. 1). The IDP employed is a genetically engineered resilin-mimetic protein polymer, Rec1-resilin that contains no sulfur containing amino acids - considered to be necessary to stabilize AuNCs.^{18,19} Native resilin is an elastomeric insect protein with near-perfect rubber-like elasticity, outstanding resilience (>92%) and long fatigue life.²⁰ Elvin *et al.* first reported the synthesis of Rec1-resilin derived from Exon 1 of the *Drosophila melanogaster* resilin gene.²¹ The primary structure of Rec1-resilin comprises 310 amino acids: 18 copies of a 15 amino acid sequence (GGRPSDSYGAPGGGN) with a molecular mass of 28.5 kDa, measured using matrix assisted laser desorption ionization time-of-flight mass spectrometry (MALDI-TOF-MS) (Fig. S1 in Supplementary Information).²¹ Recently, Dutta *et al.* demonstrated the intrinsically disordered nature of Rec1-resilin¹⁹ and its unusual multi-stimuli responsiveness (responsive to pH, temperature, ions, and light) in aqueous solutions.²² The multi-stimuli responsiveness of Rec1-resilin has also been employed to develop tuneable interfaces,²³ patterned surfaces,²⁴ and responsive hydrogels.²⁵ We have previously demonstrated a one-step synthesis of noble metal nanoparticles (NPs) using Rec1-resilin as directing agent in the presence of NaHB₄ as reducing agent.^{26,27} Here we report our discovery that under a controlled environment (pH>11) Rec1-resilin can act simultaneously as the directing agent and the reducer; and it also perform the role of a highly efficient stabilizer once AuNCs are formed.

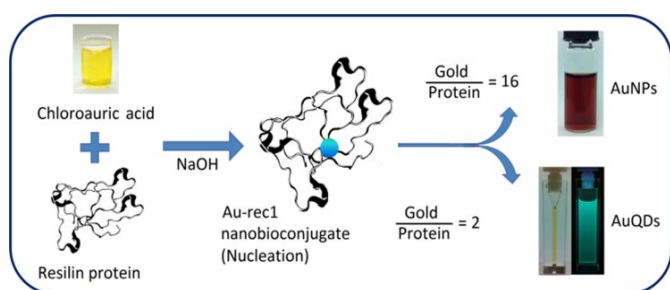


Fig. 1. Schematic of AuNPs and fluorescent AuNCs green synthesis using Rec1-resilin as a multi-functional template.

Experimental

Materials

Phosphate buffered saline (PBS, pH 7.4), sodium hydroxide (NaOH), chloroauric acid (HAuCl₄), glutathione and silver nitrate (AgNO₃) of analytical grade were purchased from Sigma-Aldrich. 18.1 MΩ-cm ultrapure MilliQ water was used for all the experiments.

Synthesis and purification of Rec1-resilin

Briefly, for Rec1-resilin synthesis, CG15920 gene (exon-1, native resilin) of the *D. melanogaster* was cloned and expressed as a water soluble protein in the bacteria *Escherichia coli*, as reported

elsewhere.²¹ The expressed protein was obtained by cell disruption and purified using a three step non-chromatographic purification method involving salt precipitation (using 20% ammonium sulphate), overnight dialysis (at 4 °C in excess phosphate-buffered saline, PBS) and heating (at 80 °C for 10 min under stirring). Any denatured protein was removed by centrifugation at 12,000 g and 20 °C for 15 min.²¹

Green synthesis of Rec1-resilin-directed AuNCs

For AuNCs synthesis, a wide range of Au: protein molar ratios (2 to 16) were examined. Typically, for Au: protein molar ratio of 16, 5 mg of Rec1-resilin was dissolved in 875 μl of 10 mM PBS with pH corrected to ~12 using 0.5 M NaOH. We have identified that at pH >11, the tyrosine (Tyr) residues in Rec1-resilin de-protonate to the tyrosinate form and thereby have the potential to generate electrons for metal ion reduction.²² About 125 μl of 40 mM HAuCl₄ was added to the above protein solution as precursor to AuNCs. The solution was then vortex mixed for 2 minutes and incubated in a quiescent condition for 10 days at 37, 50 and 70 °C in the dark to initiate AuNCs nucleation and growth. Samples were drawn successively over a regular time interval for examination.

Characterization

Steady state fluorescence excitation and emission measurements of the generated nanobioconjugates were recorded using a Cary Eclipse fluorescence spectrophotometer (Varian Inc., USA). UV-Vis absorption spectra of nanobioconjugates were recorded using an Evolution 201 UV-Vis spectrophotometer (Thermo Scientific, USA). The chemical states of AuNCs was analysed using an AXIS Ultra DLD X-ray photoelectron spectrometer (Kratos Analytical, Japan). Quantum yield and lifetime measurements of nanobioconjugates were recorded using a FLS980 fluorescence spectrophotometer (Edinburgh Instruments, UK). The secondary structure analyses of Rec1-resilin and nanobioconjugates were performed using a J815 UV-Vis CD spectrometer (JASCO analytical instruments, Japan). Mass spectra of Rec1-resilin and nanobioconjugates were obtained using ultrafleXtreme MALDI-TOF (Bruker Daltonics) operating in linear positive mode. High resolution transmission electron microscope (TEM) and scanning TEM (STEM) images of AuNCs were recorded using JEOL 2100F (at 200 kV, resolution ~2 Å) and dual-aberration corrected FEI Titan³ 80-300 (at 300 kV, resolution ~1 Å) TEM. Further details on characterization are provided in Supplementary Information.

Results and discussion

It was observed that after formation and upon equilibration, the nanobioconjugate initially showed bright blue fluorescence without any plasmon resonance. After a period of time, depending on the precursor: protein ratio and the temperature of equilibration, the nanobioconjugates displayed surface plasmon resonance, indicating formation of AuNPs. Therefore, the kinetics of fluorescent AuNCs formation and its evolution to AuNPs depends critically on the precursor protein ratio and the temperature. At lower Au: protein molar ratio of 2 (equilibrated at 50 °C), the sample exhibited bright blue fluorescence, as shown in Fig. 2A. The 3D-fluorescence

excitation-emission matrix contour plot of the sample is shown in Fig. 2B. The contour plot reveals two excitation/emission maxima (EEM) at $\sim 380/460$ nm and $\sim 325/420$ nm, respectively that correspond to Au^0 nuclei and Rec1-resilin dityrosine formation. No surface plasmon resonance was observed even after ten days of equilibration indicating stable AuNCs formation. The chemical state of the gold was assessed throughout using X-ray photoelectron spectroscopy (XPS). The Au $4f_{7/2}$ XPS spectra of blue fluorescent Rec1-resilin nanobioconjugate revealed existence of both Au^0 and Au^{1+} valence state of Au (Fig. 2C). The binding energy peak position of Au^0 $4f_{7/2}$ observed at 83.45 eV (65.5%) demonstrated positive binding energy shift relative to that of bulk Au. This shift can be attributed to increased binding energy with reduction in cluster size, supporting the formation of sub-nanometer clusters.²⁸

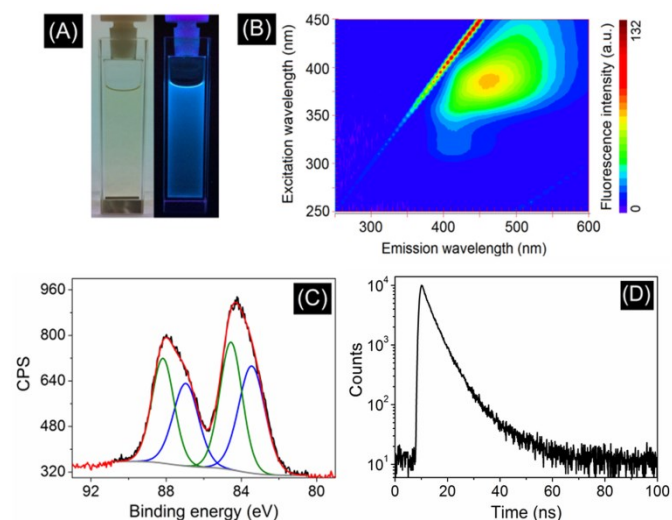


Fig. 2. (A) Photographs under visible and 365 nm UV light, (B) 3D-excitation/emission matrix contour plot, (C) Au 4f XPS spectra, and (D) Fluorescence lifetime spectra of blue fluorescent Au^0 nuclei-Rec1-resilin nanobioconjugate.

The nucleation and growth of AuNCs were shown to be dependent on the Au precursor to Rec1-resilin ratio. The evolution of AuNCs was examined in detail at different temperatures using UV-Vis spectroscopy for Au: protein molar ratio of 16 (Fig. S2 in Supplementary Information). The progressive formation of plasmonic AuNPs (diameter $\gg 2$ nm) was followed with gradual increase in the intensity of UV absorption peak (λ_{max}) at ~ 524 nm for 70 and 50 °C samples and ~ 533 nm for 37 °C sample. The kinetics of AuNPs growth was observed to enhance with increasing temperature (70 °C > 50 °C > 37 °C). We tested the hypothesis that the initial bright blue fluorescence was caused by initial stable Au^0 nuclei, which then grow into AuNCs and AuNPs. The nanobioconjugate dispersion (equilibrated for initial 24 h) was ultra-centrifuged at 10,000 rpm for 5 min to remove AuNPs formed and to obtain Au^0 nuclei in the supernatant. The 3D-fluorescence matrix contour plot (Fig. 3) of the centrifuged supernatant showed two concentric EEMs at $\sim 380/460$ nm and $\sim 325/420$ nm, respectively. This observation clearly indicates the first stable Au^0 nuclei formed to exhibit emission concentric maxima at ~ 460 nm (corresponding

to bright blue fluorescence), where the single weak concentric EEM at $\sim 325/420$ nm corresponds to Rec1-resilin's dityrosine fluorescence at the same experimental conditions (Fig. S3 in Supplementary Information).²⁹

It is presumed that the dityrosine formation in the protein template aids in AuNCs stabilization. The progressive quenching of Au^0 nuclei fluorescence with time due to AuNPs growth is shown in Fig. S4 in Supplementary Information. Fig. S5 in Supplementary Information shows the evolution of metallic gold with progressive reduction of precursor (Au^{3+}) to Au^{1+} and finally to Au^0 with the corresponding changes in the XPS intensity of Au $4f_{7/2}$ binding energies at 85.5, 84.5 and 83.0 eV, respectively. From the XPS spectra it is clear that Au^{3+} is reduced to Au^{1+} rapidly (<5 min) under the reaction conditions. However, conversion from Au^{1+} to Au^0 is relatively slower and even after 24 days of equilibration, significant amounts of Au^{1+} species (58.6%) was observed. This observation suggested a compositional mixture of an Au^0 core with surface Au^{1+} atoms.

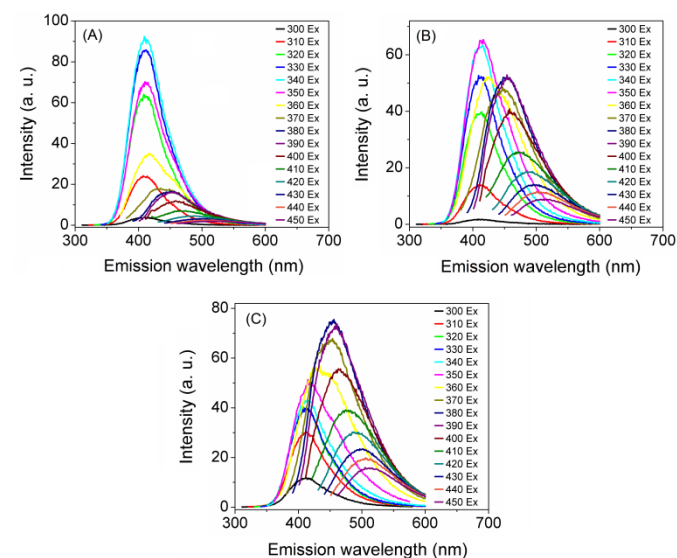


Fig. 3. Excitation-emission matrix fluorescence spectra of centrifuged AuNCs-Rec1-resilin nanobioconjugate (Au: protein molar ratio of 16 sample) supernatants after equilibration for 1 day at (a) 30 °C, (b) 50 °C, and (c) 70 °C.

The AuNCs-Rec1-resilin nanobioconjugate supernatant was further incubated at room temperature (~ 23 °C) for almost a year and examined periodically to identify further cluster growth. The incubated supernatant produced a green fluorescence after ~ 1 month of equilibration (Fig. 4A) indicating slow growth of the nucleated AuNCs. The 3D-fluorescence matrix contour plot of the nanobioconjugate displayed EEM at $\sim 380/500$ nm (Fig. 4B). Therefore, an increased Stokes shift of 0.78 eV was measured for green fluorescent AuNCs compared to 0.67 eV for blue fluorescent AuNCs. The HOMO-LUMO gap of the blue and green fluorescent AuNCs were measured to be 2.90 and 2.86 eV respectively, using Tauc plot (Section S1.3 and Fig. S7 in Supplementary Information),³⁰ and arises principally from an interband transition ($sp \leftarrow d$). This is to note that the optical properties of Au-NCs are complicated and

critically dependent on cluster size structure and reported to display multiple HOMO-LUMO transitions have been reported due to the presence of complex orbital energy diagram.^{11, 31, 32} The absolute quantum yield (QY) of the generated fluorescent AuNCs was calculated from equation 1:³³

$$QY = \frac{PN_{em}}{PN_{ab}} \dots (1),$$

where, PN_{em} and PN_{ab} are the number of emitted and absorbed photons by the fluorescent AuNCs, measured using a fluorescence spectrophotometer. The measured QY of the blue and green fluorescent AuNCs was ~2.2% and ~3.1% in aqueous medium. The blue fluorescent AuNCs-Rec1-resilin nanobioconjugate (Fig. 2D) exhibited three radiative transition lifetimes (τ): 0.74 ± 0.03 ns, 3.72 ± 0.04 ns and 10.03 ± 0.32 ns (amplitudes corresponding to 15, 72, and 13 Rel% of the emitted photons), and the green fluorescent AuNCs-Rec1-resilin nanobioconjugate (Fig. 4C) exhibited three radiative transition lifetimes of 0.61 ± 0.04 ns, 3.42 ± 0.06 ns and 8.74 ± 0.29 ns (amplitudes corresponding to 12, 69, and 19 Rel% of the emitted photons); where the first two lifetimes can be associated with dityrosine and the third with the generated AuNCs.²⁹

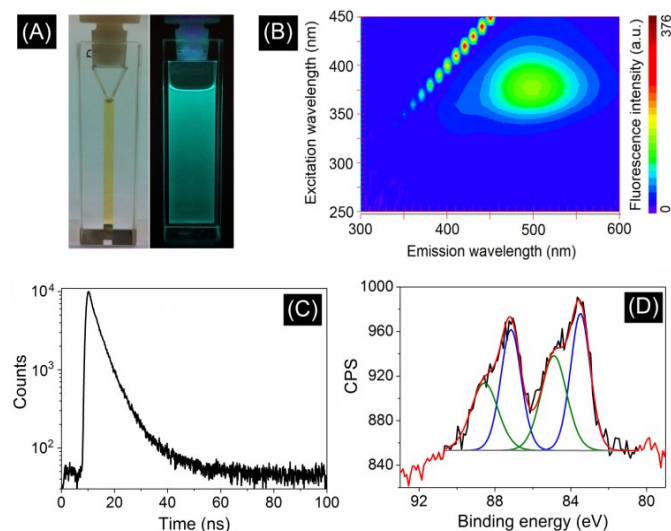


Fig. 4. (A) Photographs under visible and 365 nm UV light, (B) 3D excitation/emission contour plot, (C) Fluorescence lifetime spectra, and (D) Au 4f XPS spectra of green fluorescent AuNCs-Rec1-resilin nanobioconjugate.

The high resolution Au $4f_{7/2}$ XPS spectra of green fluorescent AuNCs nanobioconjugate revealed the existence of both Au^0 and Au^{1+} valence state with respective binding energy observed at 83.4 eV and 84.8 eV respectively (Fig. 4D). The green fluorescent AuNCs revealed an increase in Au^0 state at ~70% abundance, greater than that of freshly nucleated AuNCs (65.5%), further supporting the growth of NCs. Previous studies on AuNCs using alternative capping agents have reported ~10% to 25% abundance of the of Au^{1+} species.^{34, 35} Interestingly, no further red shift in fluorescence was observed with maturation over time and the fluorescence of

AuNCs-Rec1-resilin nanobioconjugate remained stable for almost a year (Fig. S8 in Supplementary Information). Fig.S7 in Supplementary Information depicts the UV-Vis absorbance spectra of freshly prepared blue and final green fluorescent AuNCs nanobioconjugate. It reveals no Au-plasmon resonance and confirmed no further cluster growth and thus demonstrates the robustness and stability of AuNCs formed at room temperature.

The changes in the secondary structural evolution of Rec1-resilin in the presence of Au ions were examined experimentally using circular dichroism (CD) spectroscopy. At pH 12, the measured far-UV CD spectra of Rec1-resilin (Fig. 5) displayed a large negative band with a single minimum at ~195-200 nm (due to $\pi-\pi^*$ transition) and a very low ellipticity above 215 nm. This observation suggested overall random coil characteristics of the protein.³⁶ Upon addition of Au ions (Au^{3+}) to Rec1-resilin (2:1, Au: Rec1-resilin molar ratio), only a marginal secondary structure change in ellipticity of protein was observed. This was also similar for both the blue and the green fluorescent nanobioconjugate samples (Fig. 5). Therefore, it can be concluded that Rec1-resilin being an IDP does not undergo any significant secondary structural change during synthesis and stabilization of AuNCs.

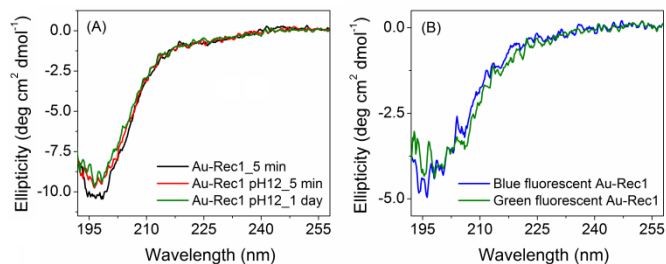


Fig. 5. CD spectra of (A) Rec1-resilin and Au: Rec1-resilin (2:1 molar ratio) solution as a function of time at pH12, (B) Corresponding fluorescent AuNCs-Rec1-resilin nanobioconjugates.

To visualize and analyse the size, structure and morphology of the AuNCs formed; high-angle annular dark-field scanning transmission electron microscopy (HAADF-STEM) imaging was performed on green fluorescent AuNCs-Rec1-resilin nanobioconjugate. The Au atoms exhibit strong Z (atomic number) contrast compared with the light atoms (mainly C) of the support film and stabilizing protein. The typical diameter of AuNCs 3D particles generated was confirmed to be <1.5 nm (Fig. 6A). At higher magnification (Fig. 6B), individual gold atoms, their dimers and diffuse atomic clusters are also revealed. Through high-resolution transmission electron microscopy (HRTEM), visible ordering consistent with the face-centred cubic (FCC) structure of bulk Au could be detected within the AuNCs (Fig. 6C, 6D & 6E). The AuNCs were observed to rotate under the electron beam: Fig. 6C & 6D show two different views of the same AuNC, which was captured along its [110] and [112] zone axes, respectively. The dark contrasts observed in HRTEM images can be interpreted as atomic columns (Fig. S9 in Supplementary Information). Twinning was also commonly observed (see red lines in Fig. 6E and extra spot in FTE of Fig. 6D). The Structural evolution of medium-sized AuNC ($n=27-35$), probed using Photoelectron spectroscopy (PES) and theoretical

calculations, demonstrated low-symmetry core-shell structures with the number of core atoms increasing with cluster size. The cluster-to-bulk transformation and the appearance of bulk-like FCC fragment is reported to start to emerge at the medium size range ($n \sim 38$).⁷ Probing the 2D to 3D structural transition in AuNC anions, using argon tagging, revealed that Au₁₂ is the crossover size from 2D to 3D structures during vapour phase deposition of Au particles. However, no such in-depth investigation has been performed on AuNCs synthesised in condensed phase.³⁷

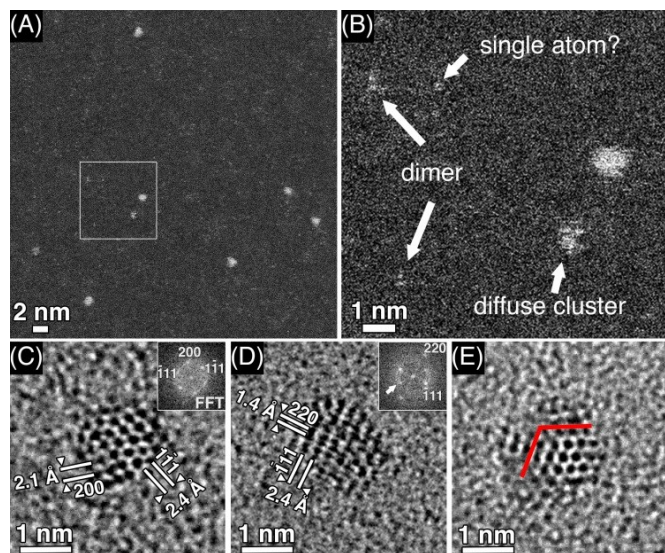


Fig. 6. (A) HAADF-STEM image of AuNCs in green fluorescent Au-Rec1-resilin nanobioconjugate. (B) Enlarged view of area framed in (A), showing a variety of Au aggregates. (C), and (D) show HRTEM images of AuNCs with FCC structure viewed along the [110] and [112] zone axis, respectively. (E) shows a AuNC with at least two [111] twins.

In order to examine the effect of pH over photo-stability of generated AuNCs-Rec1-resilin nanobioconjugate, the fluorescence characteristics of the green fluorescent AuNCs-Rec1-resilin nanobioconjugate was studied as a function of pH. The pH of the solution was adjusted in forward (pH 12 to 2) and reverse cycles (pH 2 to 12) using HCl and NaOH solution, and the change in the fluorescence intensities of both the AuNCs and the protein's dityrosine were followed. The AuNCs fluorescence intensity was observed to be reversible with pH cycling, where the fluorescence intensity decrease with decrease in pH (forward cycle) and increase with increases in pH (reverse cycle) (Fig. S10A in Supplementary Information). The emission intensity ratio of the AuNCs to dityrosine was also observed to decrease with pH (Fig. S10B in Supplementary Information). This observation indicates the transition and difference in stable states of AuNCs-Rec1-resilin nanobioconjugate with variable pH. However, no significant difference in solution state of nanobioconjugates was observed visually (Fig. S10A in Supplementary Information). The change in fluorescence property of the nanobioconjugate may be attributed to the change in the negative surface charge density (Fig. S10C in Supplementary Information) and inter-AuNCs distance. Change in

the fluorescence intensity with change in the surface negative charge density of reduced glutathione stabilized AuNCs has been reported by Ding et al.³⁸ On the other hand, photoluminescence property of semiconductor QDs has been reported to vary with inter-dot distance.³⁸ A proposed schematic of the AuNCs-Rec1-resilin nanobioconjugate at pH ~ 12 and ~ 2 is shown in Fig. S11 in Supplementary Information. MALDI-TOF-MS of AuNCs-Rec1-resilin nanobioconjugate was performed to identify the Au-cluster size, as demonstrated by many researchers for BSA protected AuNCs.¹⁵ Fig. S12 in Supplementary Information shows the MALDI-TOF-MS of synthesized green fluorescent AuNCs-Rec1-resilin nanobioconjugate and neat Rec1-resilin for comparison. MALDI-TOF-MS of green fluorescent AuNCs-Rec1-resilin nanobioconjugate showed no major peak in the range of 5,000 to 50,000 m/z suggesting fragmentation ($< 5,000$ m/z) of nanobioconjugate during the MALDI process. Such extensive core and/or ligand fragmentation, complicating formula assignments have been previously reported in literature for monodispersed AuNCs using MALDI-MS.^{40,41}

In order to examine the stability of the AuNCs in presence of foreign entities, the effect of glutathione on the stability and fluorescence of the synthesized AuNCs-Rec1-resilin nanobioconjugate, AuNCs-Rec1-resilin nanobioconjugate dispersion was incubated with glutathione (equimolar concentration to that of protein) at room temperature. The bio-thiol ligand, glutathione (GSH) is an important antioxidant and the most abundant (~ 5 mM) non-protein thiol in mammalian cells.⁴² They play a major role in many biochemical pathways including maintaining the normal reduced state of the cell, binding to heavy metals and aiding their excretion in urine or bile.⁴³ GSH interact strongly with Au through -SH group, and GSH exchange reaction has been reported in literature to synthesize and stabilize Au clusters.⁴⁴ The observation of a very slow but progressive decrease in fluorescence intensity over a period of 75 days (Fig. S13 in Supplementary Information) indicated that the GSH is being shielded by the steric hindrance of the Rec1-resilin peptide protecting layer. GSH was not been able to be easily penetrated and interact with the Au atoms on the AuNC surface. This resulted in negligible immediate effects on the fluorescence of synthesized AuNCs and demonstrates the potential of synthesized AuNCs-Rec1-resilin nanobioconjugate in bio-imaging and bio-sensor applications. The slow and progressive interference of GSH with AuNCs-Rec1-resilin nanobioconjugates is supported by evolution of hydrodynamic size distribution related to astute GSH and nanobioconjugate (Fig. S14 in Supplementary Information).

In order to study the effect of relatively small metal ions interactions with synthesized AuNCs-Rec1-resilin nanobioconjugate, Ag ions in the form of AgNO₃ (equimolar concentration to that of Au) was incubated with green fluorescent AuNCs-Rec1-resilin nanobioconjugate at room temperature. Ag ions have been reported to effectively interact with fluorescent AuNCs and quench its fluorescence due to classical energy transfer between small noble metal nanoclusters and metal ions.¹ The incubated nanobioconjugate showed only a marginal decrease in fluorescence, over a period of 55 days (Fig. S15 in Supplementary Information). The observed decrease in fluorescence could possibly be due to formation of a few alloy nanoparticles (> 2 nm) exhibiting UV/Vis absorption peaks around 480 nm. Presumably, weak penetration of Ag ions to AuNCs surface and its interaction with stabilizing Rec1-

resilin leading to increase in nanobioconjugate size and distribution, as shown in Fig. S15 in Supplementary Information.²¹ Therefore, we propose that interaction of Ag ions with AuNCs is relatively slow and hindered by the Rec1-resilin peptide protecting layer with a strong interaction between protein peptide and formed AuNC cores. This observations demonstrate the potential of synthesized robust AuNCs-Rec1-resilin nanobioconjugate for bio-imaging and sensor applications.

Conclusions

In summary, we have demonstrated a one-pot green synthesis method for preparing highly stable, fluorescent, water-dispersible quantum AuNCs using an intrinsically disordered protein (IDP) polymer as multi-functional template. This work for the first time confirms that IDPs with appropriate amino acid segments, particularly containing tyrosine residues, can serve simultaneously as ligand, directing agent, template and reducing agent for producing water-dispersible noble metal quantum clusters. This method could be potentially extended to generate other noble metal and metal-alloy quantum clusters such as platinum, silver, copper, etc., using intrinsically disordered RLPs as multi-functional templates.^{18,45} The AuNCs formed using a biocompatible IDP as reducing agent and stabilizer, renders the fluorescent AuNCs as ideal fluorophores. This work represents tantalising opportunities for tailoring AuNCs for bio-imaging, biomedical engineering, molecular biotechnology and extremely active gold catalysis.

Acknowledgements

This work was financially supported by the Australian Research Council (ARC Discovery Grants DP1092678 and DP120103537). The authors acknowledge the financial support of the Victorian State Government and Monash University for instrumentation, and use of the facilities within the Monash Centre for Electron Microscopy. The authors thank Mr. Yatin J Mage and Prof. Thomas Nann of Ian Wark Research Institute; Dr. Emma Parkinson-Lawrence, School of Pharmacy and Medical Sciences, University of South Australia for helping with lifetime measurements and CD spectroscopy.

References

- W. Chen and S. Chen, *Functional nanometer-sized clusters of transition metals: Synthesis, properties and applications*, Royal Society of Chemistry, 2014.
- Y. Lu and W. Chen, *Chem. Soc. Rev.*, 2012, **41**, 3594-3623.
- R. Jin, *Nanoscale*, 2015, **7**, 1549-1565.
- L. Shang, S. Dong and G. U. Nienhaus, *Nano Today*, 2011, **6**, 401-418.
- N. Li, P. Zhao and D. Astruc, *Angew. Chem. Int. Ed.*, 2014, **53**, 1756-1789.
- J. Oliver-Meseguer, J. R. Cabrero-Antonino, I. Domínguez, A. Leyva-Pérez and A. Corma, *Science*, 2012, **338**, 1452-1455.
- N. Shao, W. Huang, Y. Gao, L.-M. Wang, X. Li, L.-S. Wang and X. C. Zeng, *J. Am. Chem. Soc.*, 2010, **132**, 6596-6605.
- R. Huang, Y.-H. Wen, G.-F. Shao, Z.-Z. Zhu and S.-G. Sun, *RSC Adv.*, 2014, **4**, 7528-7537.
- J. Zheng, P. R. Nicovich and R. M. Dickson, *Annu. Rev. Phys. Chem.*, 2007, **58**, 409-431.
- J. Zheng, C. Zhang and R. M. Dickson, *Phys. Rev. Lett.*, 2004, **93**, 077402.
- J. Zheng, C. Zhou, M. Yu and J. Liu, *Nanoscale*, 2012, **4**, 4073-4083.
- J. Li, J.-J. Zhu and K. Xu, *TrAC, Trends Anal. Chem.*, 2014, **58**, 90-98.
- J. Xie, Y. Zheng and J. Y. Ying, *J. Am. Chem. Soc.*, 2009, **131**, 888-889.
- D. M. Chevrier, A. Chatt and P. Zhang, *J. Nanophoton.*, 2012, **6**, 064504.
- P. Lourdu Xavier, K. Chaudhari, A. Baksi and T. Pradeep, *Nano Rev.* 2012, **3**, 14764.
- Y. Xu, J. Sherwood, Y. Qin, D. Crowley, M. Bonizzoni and Y. Bao, *Nanoscale*, 2014, **6**, 1515-1524.
- Y. Li, H. Cheng, T. Yao, Z. Sun, W. Yan, Y. Jiang, Y. Xie, Y. Sun, Y. Huang, S. Liu, J. Zhang, Y. Xie, T. Hu, L. Yang, Z. Wu and S. Wei, *J. Am. Chem. Soc.*, 2012, **134**, 17997-18003.
- R. Balu, J. Whittaker, N. K. Dutta, C. M. Elvin and N. R. Choudhury, *J. Mater. Chem. B*, 2014, **2**, 5936-5947.
- R. Balu, R. Knott, N. P. Cowieson, C. M. Elvin, A. J. Hill, N. R. Choudhury and N. K. Dutta, *Sci. Rep.*, 2015, **5**, 10896.
- J. Whittaker, R. Balu, N. R. Choudhury and N. K. Dutta, *Polym. Int.*, 2014, **63**, 1545-1557.
- C. M. Elvin, A. G. Carr, M. G. Huson, J. M. Maxwell, R. D. Pearson, T. Vuocolo, N. E. Liyou, D. C. C. Wong, D. J. Merritt and N. E. Dixon, *Nature*, 2005, **437**, 999-1002.
- N. K. Dutta, M. Y. Truong, S. Mayavan, N. Roy Choudhury, C. M. Elvin, M. Kim, R. Knott, K. M. Nairn and A. J. Hill, *Angew. Chem. Int. Ed.*, 2011, **50**, 4428-4431.
- M. Y. Truong, N. K. Dutta, N. R. Choudhury, M. Kim, C. M. Elvin, A. J. Hill, B. Thierry and K. Vasilev, *Biomaterials*, 2010, **31**, 4434-4446.
- N. K. Dutta, N. R. Choudhury, M. Y. Truong, M. Kim, C. M. Elvin and A. J. Hill, *Biomaterials*, 2009, **30**, 4868-4876.
- M. Y. Truong, N. K. Dutta, N. R. Choudhury, M. Kim, C. M. Elvin, K. M. Nairn and A. J. Hill, *Biomaterials*, 2011, **32**, 8462-8473.
- S. Mayavan, N. K. Dutta, N. R. Choudhury, M. Kim, C. M. Elvin and A. J. Hill, *Biomaterials*, 2011, **32**, 2786-2796.
- WO Pat.*, WO2014071463A1, 2014.
- M. Turner, V. B. Golovko, O. P. H. Vaughan, P. Abdulkin, A. Berenguer-Murcia, M. S. Tikhov, B. F. G. Johnson and R. M. Lambert, *Nature*, 2008, **454**, 981-983.
- G. Harms, S. Pauls, J. Hedstrom and C. Johnson, *J. Fluoresc.*, 1997, **7**, 283-292.
- J. Tauc and A. Menth, *J. Non-Cryst. Solids*, 1972, **8**, 569-585.
- M. Zhu, C. M. Aikens, F. J. Hollander, G. C. Schatz and R. Jin, *J. Am. Chem. Soc.* 2008, **130**, 5883-5885.
- S. A. Miller, J. M. Womick, J. F. Parker, R. W. Murray and A. M. Moran, *J. Phys. Chem. C*, 2009, **113**, 9440-9444.
- B. Wardle, *Principles and applications of photochemistry*, Wiley, 2009.
- X. Le Guével, B. Hötzer, G. Jung, K. Hollemeyer, V. Trouillet and M. Schneider, *J. Phys. Chem. C*, 2011, **115**, 10955-10963.
- X. L. Guével, N. Daum and M. Schneider, *Nanotechnology*, 2011, **22**, 275103.
- I. Gokce, R. W. Woody, G. Anderluh and J. H. Lakey, *J. Am. Chem. Soc.*, 2005, **127**, 9700-9701.
- W. Huang and L. S. Wang, *Phys. Rev. Lett.*, 2009, **102**, 153401.
- W. Ding, Y. Liu, Y. Li, Q. Shi, H. Li, H. Xia, D. Wang and X. Tao, *RSC Adv.*, 2014, **4**, 22651.
- K. Tai, W. Lü, I. Umezū and A. Sugimura, *App. Phys. Exp.* 2010, **3**, 035202.
- J. F. Parker, C. A. Fields-Zinna and R. W. Murray, *Acc. Chem. Res.*, 2010, **43**, 1289-1296.

- 41 Y. Lu and W. Chen, *Anal. Chem.* 2015, DOI:10.1021/acs.analchem.5b00848.
- 42 A. H. Pressman and S. Buff, *Glutathione: The ultimate antioxidant*, St. Martin's Press, 1998.
- 43 J. M. Berg and J. L. Tymoczko, *Biochemistry*, Freeman & Company, 2002.
- 44 Y. Shichibu, Y. Negishi, T. Tsukuda and T. Teranishi, *J. Am. Chem. Soc.*, 2005, **127**, 13464-13465.
- 45 R. Balu, N. K. Dutta, N. R. Choudhury, C. M. Elvin, R. E. Lyons, R. Knott and A. J. Hill, *Acta Biomater.*, 2014, **10**, 4768-4777.

TOC

A multi-responsive intrinsically disordered protein (IDP)-directed green synthesis of fluorescent gold nanoclusters

Rajkamal Balu,^a Laure Bourgeois,^b Christopher M. Elvin,^c Anita J. Hill,^d Namita R. Choudhury,^{*a} and Naba K. Dutta,^{*a}

^a Ian Wark Research Institute, University of South Australia, Mawson Lakes, SA 5095, Australia.

^b Monash Centre for Electron Microscopy, Department of Materials Engineering, Monash University, Clayton, VIC 3800, Australia.

^c CSIRO Agriculture, Level 6, Queensland Bioscience Precinct, St Lucia, QLD 4067, Australia.

^d CSIRO Manufacturing, Clayton, VIC 3168, Australia.

* Correspondence E-mail: naba.dutta@unisa.edu.au; namita.choudhury@unisa.edu.au

